PERGAMON

Journal of Structural Geology 23 (2000) 507–520

JOURNAL OF STRUCTURAL GEOLOGY

www.elsevier.nl/locate/jstrugeo

Late Quaternary slip rates and slip partitioning on the Alpine Fault, New Zealand

Richard J. Norris*, Alan F. Cooper

Department of Geology, University of Otago, PO Box 56, Dunedin, New Zealand

Received 4 July 2000; accepted 20 July 2000

Abstract

Published geological data on Late Quaternary offsets on the Alpine Fault, New Zealand, have been assembled into a common format and analysed with respect to uncertainties. Uncertainties arise mainly from measurement of offset features, relating apparent offsets to actual fault slip, and dating the offset features. Despite the considerable uncertainties, the data form a coherent set consistent with a relatively constant rate of strike-slip of 27 ± 5 mm/year between Milford Sound and Hokitika. This rate represents 70–75% of the fault-parallel interplate motion. North of the confluence with the Hope Fault, the rate drops substantially. Dip-slip rates, on the other hand, show considerable variation along strike, rising to a maximum of more than 10 mm/year in the central section and decreasing to zero at the southern end. Partitioning of c. 25% of the interplate slip on to structures east of the Alpine Fault occurs in the central section, consistent with predictions from critical wedge models. The partitioning of all the fault-normal component of displacement on to other structures in the south may be related, in part, to a doubling in width of the deforming wedge to the east. Most probably, however, the fault-normal displacement is mainly accommodated by underthrusting of the Australian plate offshore, due to a change in the nature of the crust from continental to oceanic.

1. Introduction

The Alpine Fault passes down the west side of New Zealand's South Island, where it is the most obvious manifestation of the Australian–Pacific plate boundary (Fig. 1). The total rate of displacement across the plate boundary in central South Island, based on global plate tectonic data averaged over the last 3 million years, is 37 ± 2 mm/year on a bearing of 071 ± 2° (Nuvel 1A model of DeMets et al., 1994; note that errors quoted are based on the internal consistency of the model and do not take into account any systematic errors). The Australian plate is moving east–northeast relative to the Pacific plate. This motion translates to 35.5 ± 1.5 mm/year parallel to the Alpine Fault and 10 ± 1.5 mm/year perpendicular to it, making the boundary a transpressional zone. The convergence has resulted in the uplift of the Southern Alps and the exhumation of deep-seated crustal rocks immediately east of the fault during the last few million years (Norris et al., 1990).

Long-range satellite-based geodetic measurements (Larson and Fraymuller, 1995) are in close agreement with the Nuvel 1A estimates of plate motion, and recent GPS measurements within New Zealand (Beavan et al., 1999) are also consistent with these values. A more recently published pole of rotation for the Pacific/Australian plates based on GPS data (Tregoning et al., 1998) gives a higher rate parallel to the Alpine Fault, but a lower rate normal to it. Within the error limits, however, the rates are still compatible with the Nuvel 1A estimates.

The Alpine Fault was first recognised as a major fault by Wellman and Willett (1942), and the determination of total strike-slip displacement of around 480 km was reported by Wellman in 1949 (quoted in Benson, 1952). Wellman also compiled the first dataset of Late Quaternary offsets on the fault (Wellman, 1953, 1955), clearly showing it to be a highly active structure. Despite this early work, there has been ongoing debate as to the proportion of the interplate slip accommodated by the fault, and the degree of slip partitioning between the fault and other structures within and east of the Southern Alps (Suggate, 1963; Walcott, 1978a, 1998; Norris et al., 1990). Slip partitioning may involve accommodation of fractions of the total interplate slip, each with similar net directions, on a number of different structures, or it may involve splitting of the normal and parallel components between different structures (e.g. Walcott, 1978b; McCaffrey, 1991, 1992; Molnar, 1992;

* Corresponding author. Tel.: 00-64-3-479-7519; fax: 00-64-3-479-7527.
E-mail addresses: richard.norris@stonebow.otago.ac.nz (R.J. Norris), alan.cooper@stonebow.otago.ac.nz (A.F. Cooper).

0191-8141/01/$ - see front matter
PII: S0191-8141(00)00122-X

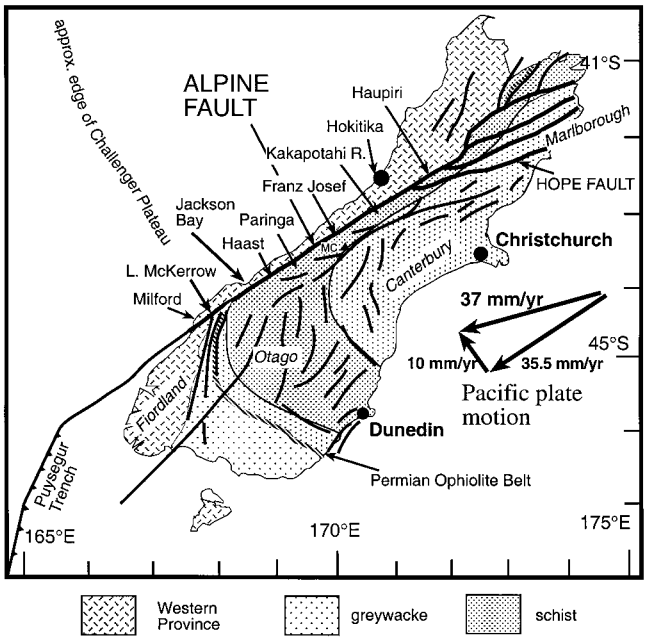

Fig. 1. Map of South Island, New Zealand, showing regional geology and general localities referred to in the text. Figs. 2 and 3 show specific localities of observations. The Alpine Fault is shown by a heavy line; lighter lines are other faults thought to be active in the Quaternary. Due to restrictions of scale, faults shown are somewhat generalised in order to show style and distribution of Quaternary deformation. MC: Mount Cook (3764 m), the highest point of the Southern Alps; SWFZ: South Westland Fault Zone. The interplate velocity vector shown is calculated for Franz Josef from the Nuvel 1A model of DeMets et al. (1994).

Platt, 1993; Tikoff and Teyssier, 1994). Whether either or both these styles of slip partitioning are occurring in the South Island has been a subject of some speculation (e.g. Koons, 1994; Braun and Beaumont, 1995; Teyssier et al., 1995). As the South Island has become known worldwide as an active transpressional orogen, comparisons with other zones of deformation have increased (e.g. Teyssier et al., 1995; Braun and Beaumont, 1995; Koons, 1994, 1995; Yeats and Berryman, 1987). Transpression is widely recognised as an important kinematic model in many ancient orogens (e.g. Holdsworth and Strachan, 1991; Cobbold et al., 1991), so the nature of slip partitioning within the Alpine Fault system has significant implications for understanding the mechanics of orogenic deformation.

Work on the Alpine Fault over the last 20 years has provided much information on the rates of Late Quaternary displacement on various sections of the fault (e.g. Berryman et al., 1992; Sutherland and Norris, 1995). This type of data is difficult to obtain and subject to considerable uncertainty, but sufficient data are now available to address some of the questions outlined above. Although much of the data is published, it is spread throughout the geological literature. It seems an opportune time to summarise and review the data on Late Quaternary slip rates, particularly with the completion of the SIGHT project, which obtained a variety of geophysical data across the whole South Island (Davey et al., 1998). Data from the SIGHT project will allow a detailed interpretation of crustal structure across the orogen. Early geodetic survey data on current strain rates (Walcott, 1978a; Bibby et al., 1986; Pearson, 1994) have been supplemented by a comprehensive GPS network, the results of which are allowing provisional calculation of the current velocity field across the South Island (Henderson et al., 1999; Beavan et al., 1999). Comparison of short- and long-term rates and strain distributions are crucial for understanding the dynamics of the plate boundary.

2. Alpine Fault structure

The Alpine Fault is an amazingly linear structure when viewed on a satellite photograph. In the central section of the fault, however, between Haast and Hokitika (Fig. 1), the fault in detail commonly consists of more northerly striking sections which exhibit oblique thrusting, and more easterly striking sections which are dominantly dextral strike-slip, on the scale of a few kilometres (Norris and Cooper, 1995). Seismic reflection imaging of the fault at depth also shows a feature dipping southeast at c. 50° to depths of around 25 km (Davey et al., 1995), which is about the depth from which high-grade metamorphic rocks have been exhumed in the hanging wall of the fault (Cooper, 1980; Norris et al., 1990; Grapes and Watanabe, 1992, 1994). The overall displacement across the fault here is clearly transpressional, with components of strike-slip and dip-slip. South of Haast, the fault becomes a straight, steeply dipping structure with dominantly strike-slip displacement (Berryman et al., 1992; Sutherland and Norris, 1995). North of Hokitika,

the fault splays into the more easterly striking faults of the Marlborough Fault System (Fig. 1), which progressively accommodate the plate boundary displacement.

The Southern Alps rise up immediately east of the Alpine Fault and reach their highest elevation at Mount Cook (3764 m) in the central portion of the range. East of the Main Divide, the topography becomes progressively lower towards the coast. A large number of generally west-dipping reverse faults create northeast to north trending ranges (Cox and Findlay, 1995). These extend eastwards about 100 km in the central part of the Alps, but continue for 200 km as far as the east coast in Otago (e.g. Jackson et al., 1996) (Fig. 1). Together with the Alpine Fault, they define a two-sided deforming wedge (Koons, 1990, 1994).

3. Problems and uncertainties in determining rates of offset

In order to determine a slip rate across a fault, some displaced feature is required. In general, vertical displacement rates, involving offset of a horizontal surface, are easier to determine than horizontal offsets, which require the identification and dating of an offset linear feature. In addition, uplift rates may be determined from raised deposits whose original position relative to sea level is known. To convert this to a vertical offset rate, the rate of uplift of the "downthrown" side of the fault is required. Dip-slip rates may be obtained from vertical offsets if the dip of the fault is known. In many places, the Alpine Fault dips at around 30°SE, and dip-slip may be measured directly in outcrop. Care must be taken to distinguish between slip and separation. Where the slip direction is known, e.g. from slickenside striations on the fault surface, components of slip may be calculated (assuming that the striations are representative of the net slip direction).

Uncertainties associated with determining rates of slip may be grouped under two principal headings. Firstly, there is the uncertainty in measuring the true fault-related offset of a feature, and secondly there is the uncertainty in assigning an age to the feature. In many cases, these uncertainties are not normally distributed about a mean value but show highly skewed distributions resulting in maximum or minimum estimates. In many cases, they are difficult to quantify.

3.1. Uncertainties in measuring amount of offset

In the case of a clearly displaced feature such as a terrace surface or stream channel, actual measurement of the offset may simply be a case of field measurement using surveying instruments or a tape measure and can be accomplished with negligible errors. Uncertainties arise, however, in ascertaining the relationship between the offset feature and fault slip. For instance, a steam channel may be irregular and may show erosion or lateral migration since offset occurred. In this respect, a dry channel may be a better marker than an active channel, although on the high rainfall West Coast, most channels are active.

A terrace surface may have continued to accumulate sediment on the downthrown side of the fault after displacement commenced, or alternatively, the upthrown surface may have been degraded. In either case, the result will be a minimum estimate of fault offset. Similarly, an offset terrace riser may have been eroded back laterally following initial onset of displacement, leading to over- or under-estimates of fault offset. Lensen (1964, 1968) provided a comprehensive discussion of the problems associated with offset terrace measurements.

Where dip-slip is measured in cross-sections of the fault, the result is commonly a minimum unless a distinct offset line is observed. This is because, in most situations, only the minimum distance of overthrusting of a dated deposit can be measured. If slip direction as measured by striations on the fault plane is used to calculate fault slip, the error associated with these measurements may be significant, particularly in the case of the Alpine Fault, where the pitch of the striations is less than 45°.

3.2. Uncertainties in determining age of offset

In most cases, a sedimentary deposit has been dated using radiocarbon methods. The date itself has an analytical error associated with it. In order to calculate rates, calendric years rather than carbon years are required. Where the authors have not made this conversion, we have done so using the computer programme of Stuiver and Reimer (1993), based on published calibrations of the radocarbon time scale (e.g. Stuiver and Reimer, 1993; Stuiver and Becker, 1993; Bard et al., 1990, 1993). In addition to the quoted uncertainties (at 1σ), there are also potential additional errors in the calibration, particularly for dates $>10{,}000$ years BP (e.g. Bard et al., 1990). We have not calibrated radiocarbon ages older than 15,000 years BP.

In central Westland, there are two major suites of fluvioglacial gravels and moraine (Warren, 1967; Suggate, 1990). The older, termed the Okarito Formation (Warren, 1967), is correlated with Oxygen-isotope Stage 4 (Suggate, 1990) dated at c. 65 ± 5 ka (Martinson et al., 1987), and the younger, the Moana Formation, is the product of the last advance at c. 15 ± 2 ka (Suggate, 1990). In some cases, ages of deposits have been estimated by stratigraphic correlation with the regional glacial sequences. Provided the correlations are correct, the uncertainties in assigning dates to units based on regional stratigraphic correlation do not add large uncertainties (i.e. only of the order of $\pm 10\%$) to estimates of slip rates, due mainly to the length of time involved.

A further, commonly larger, source of uncertainty is in relating the dated material to the age of displacement. In many cases, the dated material may come from sediments well below the offset terrace or other feature, thus only allowing a maximum age (and hence minimum rate) to be

assigned. The uncertainty can rarely be quantified and we have generally indicated it by stating a minimum rate.

3.3. Uncertainties in measuring uplift rates

Uplift rates refer to the vertical motion of rocks. To measure them, a datum level is required which is usually present day sea level. Some characteristic of the deposit or feature is required which allows its original position relative to sea level to be ascertained, e.g. a shore-line deposit, intertidal shelly fauna, etc. Errors in measuring the present height of the feature are usually insignificant compared with the other uncertainties involved. These include the error in determining the original height with respect to sea level, the uncertainty in the age of the deposit, and the correction for past sea level height compared with the present. These problems are discussed in relation to Alpine Fault uplift by Hull and Berryman (1986) and Simpson et al. (1994). Note that uplift rate and dip-slip rate are different, as uplift rate includes any uplift of the "downthrown" side of the fault, as well as differential displacement across it.

3.4. Estimation of uncertainty in this paper

In the compilation of data presented in Appendix A, we have attempted to derive values for uncertainty from the available data. In the case of ^{14}C ages, this is the analytical or calibration error. For many measurements, however, a rigorously determined statistical error is not possible to determine. For instance, in correlation of a date with a feature, or where offset features bracket the real value, uncertainties are based both on calculated errors and estimated uncertainties. Errors have been propagated through calculations where possible, however. We adopt a "best estimate" based on the available data at each locality, including qualitative as well as quantitative considerations.

4. Regional rates of movement

Prominent topographic features offset along the Alpine Fault system were identified from aerial photographs, their displacements estimated and all relevant information tabulated by Wellman (1953). However, difficulties in determining the age of the displaced feature have hindered quantitative assessment of rates of displacement on the fault, and the first fully quantitative estimates were finally made at Paringa River in 1968. Based on displacement of fossiliferous Holocene marine silts, Suggate (1968) determined an uplift rate on the Alpine Fault of 35 feet/1000 years (10.7 mm/year). We now believe this value is appropriate only at a very localised upthrust ridge within the fault zone (where rates may reach 13.7 mm/year), superimposed on a broad regional uplift rate of only 7–8 mm/year (Wellman, 1979; Simpson et al., 1994).

In 1979, Wellman published an uplift map of the South Island, based on a variety of estimates of varying degrees of reliability, including tilted lake shorelines, and heights of marine benches and river terraces. Uplift rates on the Alpine Fault were shown as attaining a maximum rate slightly in excess of 10 mm/year in central Westland, decreasing both to the southwest and northeast. Adams (1980) published a slightly revised version of Wellman's map, but with the maximum uplift rate in central Westland estimated to be in excess of 20 mm/year.

Cooper and Bishop (1979) suggested that level benches occurring on schist ridges rising towards the crest of the Southern Alps from the Alpine Fault scarp represented remnants of uplifted marine terraces. A regional survey along the length of the Alpine front by Bull and Cooper (1986) used the number of inferred terraces and their altitudinal spacing to correlate with the global sequence of interglacial high sea level stands. Using these assumptions and correlations, Bull and Cooper (1986) deduced uplift rates on the Alpine Fault which reached maximum values of 8 mm/year in central Westland, decreasing to 5–6 mm/year in the northeast (Kanieri) and southwest (Haast). Ward (1988) criticised the identification of the terraces as marine, and Pillans (1990) demonstrated that the method of correlation of the terraces with the New Guinea sequence is questionable, and in particular that the marked change in rate at c. 130 ka is an artifact of the method. Nevertheless, the uplift rates determined by Bull and Cooper (1986) are compatible with rates determined independently. Using a similar correlation technique [subject to the same criticisms of Pillans (1990) as the methods of Bull and Cooper] on the spectacular terrace flights incised on to the southwest Fiordland coastline, immediately inland from the trace of the Alpine Fault, Bishop (1991) determined uplift rates of 3 mm/year.

A regional fission track study of samples from the Southern Alps has determined that exhumation rates based on reset zircon ages have accelerated with time to reach a maximum, calculated over the past 0.9 Ma, of 9 mm/year close to the Alpine Fault in the Fox Glacier–Mount Cook region (Tippett and Kamp, 1993). Uplift (= exhumation) rates decrease to the north, south and east, with contoured uplift pattern being similar in geometry and uplift rates similar in magnitude to those proposed by Wellman (1979).

5. Late Quaternary slip rate patterns

Table 1 and Appendix A list Late Quaternary slip rate determinations which have been published or are available in reports, etc. We have separated them into dip-slip, strike-slip and uplift rates. Fig. 1 shows the regional geology and many of the localities mentioned in the text, whereas Figs. 2 and 3 show all localities where strike-slip and dip-slip rates respectively have been reported. As noted above, we have re-calculated some of them using calibrated calendric dates, and attempted to provide an estimate of uncertainty. We have also listed our "best estimate" of the slip rate which

Table 1
Summary of slip rate determinations: localities are shown in Figs. 2 and 3

Locality	Type of data	Age[a](Cal BP)	Dip-slip rate[b](mm/year)	Strike-slip rate[b](mm/year)	Uplift rate (mm/year)
1) Haupiri River	Offset terrace surface, channels and terrace riser	2100 ± 250	⩾ 2.5	⩾ 6.3	
2) Inchbonnie	Offset terrace surface and offset channels	1200 ± 100	6 ± 2	10 ± 2	
3) Toaroha River	Offset terrace surface	2800 ± 400	7.8 ± 1		
4) Kaka Creek (Mikonui R.)	Mylonite thrust over stream gravels	2600–3350 interval (750 ± 116)	> 6.7		
5) Kakapotahi River	Offset river terraces and risers	13,600 ± 1200 and 7600 ± 1400	6 ± 1	29 ± 6	
6) Gaunt Creek (Waitangitaona R.)	Mylonite thrust over gravel sequences; fault plane striations	14,880 ± 200 and 12,150 ± 250	> 12	> 22	
7) Waikukupa River	Mylonite thrust over gravel sequences; fault plane striations	c. 65,000 ± 5000 and c. 15,000 ± 2000	8 ± 3	27 ± 5	
8) Paringa River	Uplifted post-glacial marine/ terrestrial sediments	15,700 ± 700	7.5 ± 1.5		8 ± 1
9) Haast River, north bank	Offset terrace surface and offset stream channel	< 4400 ± 100	> 2	> 21	
10) Haast River, south bank	Offset terrace surface and offset channel	800 ± 50	2.25 ± 0.5	28 ± 4	
11) Okuru River	Uplifted marine sediments	10,960 + 113/−411	3 ± 0.5		4 ± 0.2
12) Hokuri Creek (L. McKerrow)	Offset moraine; uplifted shells; horizontal fault plane striations	17,000 ± 2000 (moraine) 6490 ± 90 (shells)	0	26 ± 6	1.4 ± 0.5 (NW of Fault)
13) L. McKerrow	Offset walls of glacial valley uplifted intertidal shell beds	15,600 ± 110 shells: 7820–8100 (NW); 4060–4240 (SE)	< 1	26 ± 7	2.2 ± 0.2 (NW) 1.6 ± 0.3 (SE)

[a] Ages given are best estimates in calendric years BP.
[b] Slip rates are best estimates based on data available. For more details on uncertainties, assumptions, ranges of possible slip rates, and for references to published data, see Appendix A.

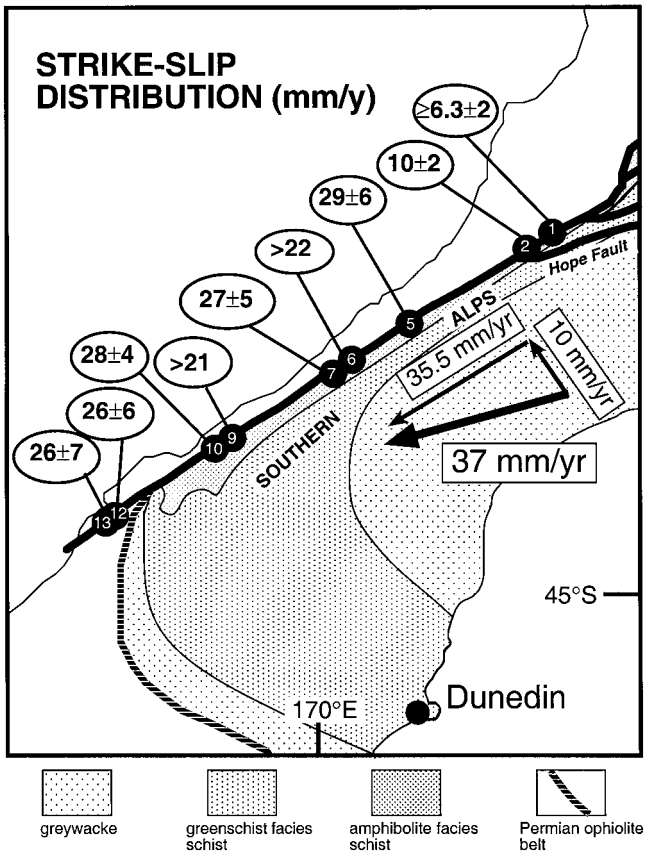

Fig. 2. Map showing localities of strike-slip rate determination. The value given in oval at each locality is the best estimate of slip rate in mm/year. The numbers in the black circles refer to the localities listed in Table 1 and Appendix A. For more details, refer to Table 1 and Appendix A.

takes into account the various levels of uncertainty. This value is based on our analysis of the reported data; for a full range of reported rates refer to Appendix A. It is the "best estimates" that we discuss below and plot in Figs. 2 and 3.

5.1. Strike-slip rates

Strike-slip rates over the past 50,000 years show no significant variation along the length of the fault south of its confluence with the Hope fault (Fig. 2). All are compatible with an average rate of 27 ± 5 mm/year. This is identical to the longer term minimum rate of 27 ± 4 mm/year estimated by Sutherland (1994) from offset sedimentary deposits in northern Fiordland. It represents 75% of the calculated interplate slip vector parallel to the Alpine Fault of 35.5 ± 1.5 mm/year (DeMets et al., 1994; Walcott, 1998). The balance is presumably distributed among the many smaller faults, mainly to the east of the Alpine Fault. These geologically determined slip rates are compatible with recent GPS surveys which show that more than 60% of the total strain across the Island is concentrated within a band from 5 km NW to 20 km SE of the Alpine Fault. The strain can be modelled as elastic strain above the SE-dipping fault zone locked at c. 8 km depth (Beavan et al., 1999).

At Haast, two trenches excavated across the recent trace of the Alpine Fault show clear evidence for three ground ruptures within the last 800 ± 50 years (Berryman et al., 1998). The total strike offset recorded by these events is 25 m, which provides a short-term strike-slip rate of 24–32 mm/year, depending on when the next rupture occurs. Provided it happens within the next 100 years, as strongly indicated by palaeoseismic data (Berryman et al., 1998; Yetton et al., 1998), a strike-slip rate of 28 ± 4 mm/year is indicated. This estimate is closely comparable to the Late Quaternary rates, to the long-term rate of Sutherland (1994), and to the rate of strain accumulation over the last 4–6 years as revealed by GPS measurements (Beavan et al., 1999). These data are consistent with the accumulation of elastic strain in the crust and its release during rupture events on the Alpine Fault.

Where precisely the balance of the strike-parallel plate boundary displacement is accommodated is not entirely clear. Some of the balance may occur within the Alpine Fault zone itself, which extends eastward from the fault for several hundred metres. Certainly there are many minor faults, many with sub-horizontal striations, or with development of pseudotachylyte (Sibson et al., 1979; Norris

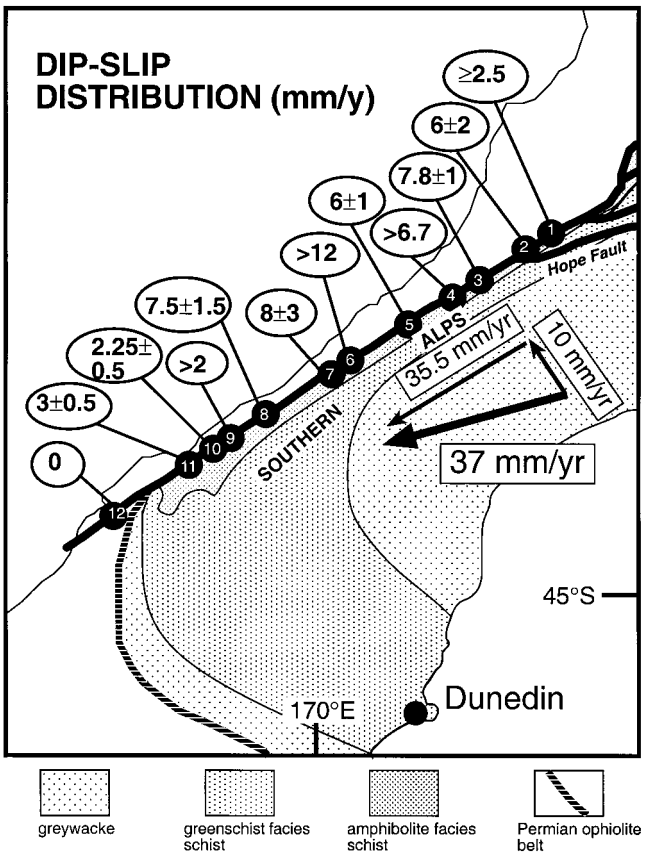

Fig. 3. Map showing localities of dip-slip rate determination. The value given in oval at each locality is the best estimate of slip rate in mm/year. The numbers in the black circles refer to the localities listed in Table 1 and Appendix A. For more details, refer to Table 1 and Appendix A.

and Cooper, 1986), within this zone that have taken up some of the displacement. Some of the offset measurements listed in Table 1, however, are offsets across the whole fault zone (e.g. Lake McKerrow; Sutherland and Norris, 1995). The South Westland Fault Zone is a major structure running parallel to the Alpine Fault and partly offshore (Fig. 1; Nathan et al., 1986). Mid-Tertiary sedimentary strata are offset across it, but there is little evidence for Quaternary displacement (Sutherland, 1995) and total offset appears to diminish northwards. Current seismicity (Eberhart-Phillips, 1995) and geodetic strain (Beavan et al., 1999) are concentrated east of the Alpine Fault in central Westland, also suggesting that the South Westland Fault Zone is not currently accommodating significant strike-slip displacement. Strike-slip displacements have been recorded on faults on the eastern side of the Alps (e.g. Cox and Findlay, 1995), but there is no quantitative assessment of their total contribution.

North of the confluence with the Hope Fault, the strike-slip rates reduce rapidly (Inchbonnie and Haupiri estimates). This is compatible with much of the slip being partitioned on to the Hope Fault (Berryman et al., 1992), which is estimated to accommodate an average horizontal slip rate of up to 23 mm/year (Cowan and McGlone, 1991), and other parallel faults.

5.2. Dip-slip rates

Estimates of dip-slip are more numerous than strike-slip, due to reasons discussed earlier. They contrast with the strike-slip estimates in showing distinct and systematic changes along the length of the fault (Fig. 3). The highest rates of 8–12 mm/year are found in the area west of Mount Cook, the highest part of the Southern Alps. Between the Paringa River and the Hope Fault confluence, they remain high at 6 mm/year or more. In fact, within the error limits, this whole section of the fault is broadly similar with a high rate of dip-slip. South of the Paringa River, however, the dip-slip rate falls away to become zero south of Jackson Bay.

The change in dip-slip rates to the south corresponds with a change in the character of the fault at the surface. In the central section, it shows a characteristic right-stepping pattern with more northerly striking oblique thrust segments dipping moderately southeast, and more easterly striking dextral strike-slip segments on the scale of a few kilometres (Norris and Cooper, 1995). This pattern has been interpreted as due to "serial" partitioning of oblique slip on the fault controlled by erosional processes at the Earth's surface (Norris and Cooper, 1995, 1997). South of Haast, however, the fault is straight, with few segments, and where seen in

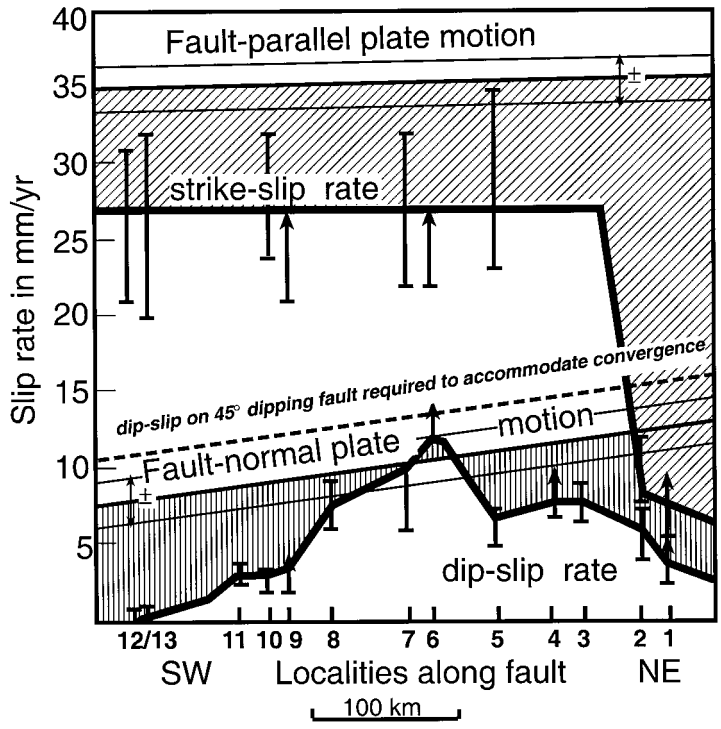

Fig. 4. Diagram showing variation of strike-slip and dip-slip rates with distance along the fault. The estimated values at each locality (numbered as in Table 1 and Appendix A) are shown as vertical bars. Minimum values are shown with an arrow at the upper end. A "best-fit" line representing the changing slip rate along the fault is shown in heavy black. The fault-parallel and fault-normal components of the interplate slip vector are also shown, as calculated from the Nuvel-1 pole (DeMets et al., 1994), together with uncertainties (shown as thin lines either side of the mean value line). The difference between the fault slip and the interplate slip is hatched and is a rough guide to the degree of partitioning. Note, however, that the fault-normal component and the dip-slip rate are not directly equivalent, as the fault-normal convergence represented by the dip-slip will be less. An estimate of the dip-slip rate required to accommodate all fault-normal displacement on a 45° dipping fault is shown by the heavy dashed line (see text for discussion).

outcrop, is a steeply dipping structure (Berryman et al., 1992; Sutherland and Norris, 1995). Striations on the fault plane in the central section are oblique to the average strike of the fault and record a distinctly oblique-slip character, whereas south of Haast, striations are sub-parallel to strike, indicating dominantly strike-slip displacement (Berryman et al., 1992; Sutherland and Norris, 1995; Norris and Cooper, 1997).

The maximum values of dip-slip within the central part of the Southern Alps have similar values to the total interplate convergence rate of 10 mm/year (DeMets et al., 1994). However, as the fault in this section dips at around 45° (Sibson et al., 1979; Norris et al., 1990), this only represents part of the total horizontal convergence (around 70%; Fig. 4). As with the strike-slip, a portion of the boundary-normal movement is accommodated by the thickening and uplift of the Southern Alps on faults east of the Alpine Fault (e.g. Cox and Findlay, 1995). The net-slip on this central part of the fault is therefore approximately consistent in direction with the interplate slip vector, but is only around 70–75% in value, with the remainder partitioned mainly to the east.

South of Jackson Bay, virtually all of the boundary-normal component of the interplate slip vector is inferred to be partitioned on to other structures either east or west of the Alpine Fault. In the transition zone between Paringa and Jackson Bay, the dip-slip component gradually reduces to zero. Although the fault-normal component of the interplate slip vector reduces southwards due to a reduction in convergence angle and a reduction in total slip rate (Fig. 4), this change is much less than the change in dip-slip rate on the fault. An increasing amount of partitioning of convergence on to other structures must therefore take place south-westwards along the fault trace.

6. Slip partitioning

Slip partitioning along plate boundaries has been described for many years (e.g. Fitch, 1972), initially along subduction boundaries where components of plate-normal and plate-parallel motion are accommodated on different structures (e.g. Walcott, 1978b; McCaffrey, 1991). Jones and Wesnousky (1992) discussed slip partitioning along the San Andreas Fault and pointed out that a complete gradation exists between complete separation and no separation of normal and parallel components on to different structures. Thus, in many cases, all faults within the system may exhibit oblique slip, with one perhaps more dominantly strike-slip and others more dominantly dip-slip. In discussing slip partitioning on the Alpine Fault, we deal with two

aspects. Firstly, how much of the total plate motion is accommodated on the Alpine Fault and how much is partitioned on to other structures within the plate boundary zone? Secondly, to what degree are the fault-normal and fault-parallel components partitioned on to different structures?

6.1. Partitioning of total displacement

In the discussion of slip rates above, we tentatively concluded that both types of slip partitioning occur in the South Island plate boundary zone. Whereas the presence of active faults and deformation throughout much of the South Island clearly indicates that not all plate boundary deformation occurs on the Alpine Fault, the degree of partitioning is more difficult to assess. The error bars on the slip rate estimates are quite large, and uncertainties in the interplate slip vector add to the problem. As noted above, the error bars on geodetically determined poles of rotation for the Pacific and Australian plates are still relatively large and calculated values for interplate displacement rates in New Zealand are compatible with the longer term average provided by Nuvel 1A (DeMets et al., 1994). The uncertainties in average strike-slip rate on the Alpine Fault reported above (27 ± 5 mm/year) and in Nuvel 1A fault-parallel motion (35.5 ± 1.5 mm/year) almost, but not quite, overlap. Thus, we may conclude that at least a small component of the fault-parallel slip is partitioned away from the fault. The data are insufficiently precise at present to determine the exact proportion; the average data indicate that c. 25% of the strike-parallel plate motion is accommodated on structures other than the Alpine Fault, but this has an uncertainty of $\pm 15\%$.

The amount of plate boundary slip partitioned on to structures east of the Alpine Fault has considerable implications for seismic hazard. Recent palaeoseismological work on the Alpine Fault (Berryman et al., 1998; Wells et al., 1999) has shown that the fault ruptures by up to 8 m in events every 100–300 years. Little is known, however, about the seismic behaviour of the large number of faults east of the Alpine Fault. This is partly because each has long return periods between events and the size of ruptures is only c. 25% or less of the Alpine Fault ruptures (e.g. Van Dissen et al., 1993). Nevertheless, if 25% of the plate boundary slip is partitioned on to this array of faults, at least one fault must rupture in every section east of the Alpine Fault during one return period on the latter. Although the size of earthquakes will be much smaller than an Alpine Fault rupture (M7–7.5 compared with M7.8–8), the total number of events will be considerably greater and each will still represent a significant hazard, especially as the specific fault that breaks is not predictable.

6.2. Partitioning of fault-normal displacement

In addition to the partitioning of a portion of the plate boundary slip away from the Alpine Fault, there is clear evidence in the slip rate data for an increasing partitioning southwards of the fault-normal component on to other structures. As noted above, the interplate slip vector changes progressively along the plate boundary due to changing distance from the pole of rotation. Using the Nuvel-1A pole of DeMets et al. (1994), the angle between the interplate vector and the Alpine Fault changes from 19° at the north end (locality 1) through 16° in the centre (locality 6) to 12° at the southern end (Milford Sound). The change results in a decreasing value of fault-normal motion southwards, from 13 mm/year near Hokitika to 7.5 mm/year at Milford Sound. Although significant, these changes are much less than the observed changes in dip-slip (Fig. 4), and slip partitioning of some sort is required. In contrast, the fault-parallel component scarcely changes along the length of the fault.

The structures currently accommodating the fault-normal component of interplate displacement have not been unequivocally identified. The area around Haast, where values of dip-slip rate on the Alpine Fault change rapidly, corresponds eastwards to a doubling of the width of the deforming zone. In the central part of the Southern Alps in Canterbury, the deforming wedge is approximately 100 km wide. In Otago, however, active reverse faults extend to the coast at Dunedin, forming the NE-oriented Otago range and basin topography and a developing fold-thrust belt (Yeats, 1987; Jackson et al., 1996; Markley and Norris, 1999). The amount of shortening represented by the NE–SW-trending Otago ranges is difficult to estimate. Over the eastern half of the island, however, the mountains are flat-topped due to the exhumation of a Cretaceous–Tertiary peneplain surface (Bishop, 1994). A rough estimate of the cumulative offset of this surface across the faulted ranges is c. 4000 m. This displacement has taken place during the Pleistocene (Youngson et al., 1998), giving a maximum rate of shortening over the past 2 Ma of 2 mm/year, assuming the rates have remained uniform. Clearly, this alone is insufficient to account for the dramatic decrease in dip-slip component on the Alpine Fault, although it may be associated with it. The widening of the deforming wedge across Otago corresponds to the outcrop of Mesozoic schists (Fig. 1) and may be related to changes in the rheology of the crust. Detailed modelling is currently being undertaken (Koons et al., 1998) to investigate the mechanics of the deformation.

Uplift and exhumation of the south-eastern side of the Alpine Fault south of Haast is evident from the mountainous terrain and the occurrence of mylonite and schist. Thus, the long-term behaviour here still includes a component of dip-slip, despite the Late Quaternary data indicating almost pure strike-slip. The change in character may therefore be relatively recent. One factor that is probably important is the change from continental crust of the Challenger Plateau on the western side to oceanic crust of the Tasman Sea. This change takes place at present in the vicinity of Jackson Bay (Fig. 1), although at earlier times it would have been progressively further southwest. Off the Fiordland coast, there is clear evidence for the partitioning of motion into

oceanward-verging thrusts to the west and strike-slip along the Alpine Fault (Davey and Smith, 1983; Cutress et al., 1998; Barnes et al., 1999). Current seismicity north of Haast is largely restricted to areas east of the Alpine Fault, whereas to the south the seismicity extends well to the west of the fault (Anderson and Webb, 1994; Eberhart-Phillips, 1995). Much of the missing normal component of plate motion may thus be partitioned into thrusting offshore. A well-developed subduction zone is not evident, however, until the Puysegur Trench some distance south of the Fiordland coast (Fig. 1; Delteil et al., 1996).

6.3. Discussion

The Late Quaternary slip rate data indicate that some degree of partitioning of plate boundary displacement occurs between the Alpine Fault and structures to the east or west. The nature of this partitioning, however, varies along the fault (Fig. 4). In the far north, much of the displacement is taken up on the Marlborough Fault System and the slip rates on the Alpine Fault decrease rapidly as a result. Anderson et al. (1993) argue for partitioning of some boundary-normal displacement on to faults west of the Alpine–Marlborough system, responsible for two large earthquakes last century. In the central part, the slip on the Alpine Fault is roughly parallel to the plate motion, with approximately 25% being accommodated within the Southern Alps east of the fault. South of Haast, the fault-normal component of displacement decreases to zero, so that partitioning of normal and parallel components takes place (Fig. 4). This change in partitioning behaviour along the fault indicates that, even along a straight structure, strain gradients parallel to the structure are not necessarily constant. Change in the amount of fault-normal displacement being partitioned along the length of the fault should result over time in the rotation of the fault trace and probably the development of a bend. This is evident in the northern part of the island (Anderson et al., 1993), but less clear in the south.

Several authors (e.g. Braun and Beaumont, 1995; Teyssier et al., 1995) have argued that the degree of partitioning of the strike-parallel and strike-normal components on to separate structures within a transpressional orogen depends on the angle of obliquity of the convergence. The degree of partitioning of fault-normal displacement on the Alpine Fault does indeed increase with increasing obliquity of convergence. The critical values of obliquity quoted by Braun and Beaumont (1995), for example, are however considerably less than those on the Alpine Fault.

Another factor controlling partitioning may be the crustal rheology and total displacement on a fault. For instance, rapid exhumation results in thermal weakening at depth (Koons, 1987) and localisation of oblique slip on to a single structure (Koons et al., 1998). Jones and Wesnousky (1992) argue that, along the San Andreas Fault, the degree of partitioning of fault-normal slip depends mainly on the angle of dip of the thrust fault. This itself, however, may be a function of the rheology and kinematics of the fault system. The precise way in which the mechanics of the deforming orogen are controlled by the interplate motion, total displacement and crustal rheology has yet to be elucidated. We do not intend to speculate further here. We conclude that the geological data show that slip partitioning occurs along the Alpine Fault, but that its style varies according to location, and may be related to plate kinematics, rates of exhumation and changes in behaviour of the crust on either side of the fault.

Acknowledgements

We thank Craig Wright, Rupert Sutherland and Guy Simpson for their assistance and ideas with some of the original work in Westland, Peter Koons and Chris Pearson for general discussions and for assistance with references to geodetic data, Donna Eberhart-Phillips for discussions on seismicity, and particularly to Kelvin Berryman for a careful and constructive review. We also thank members of the SIGHT team who pointed out the value of a review of these data. The work was funded by contracts UOO609 and UOO814 from the Public Good Science Fund of New Zealand, and by grants from the University of Otago Research Committee.

Appendix A. Catalogue of sites of published Late Quaternary slip rate estimates

The following list has been compiled from papers and reports. If uncertainties were not allocated in the original work, we have attempted to provide some quantitative assessment based on information given. We have also converted ^{14}C ages to calendric ages using the Radiocarbon Calibration Program (Quaternary Isotope Laboratory, University of Washington) in conjunction with Stuiver and Reimer (1993) and Bard et al. (1990, 1993). The localities are shown in Figs. 2 and 3. Unless otherwise stated, the analytical errors stated are 1σ.

Locality 1: Haupiri River**. Offset feature(s):** terrace surface offset vertically by 5 m, channels on surface and terrace risers displaced dextrally by 11 ± 2 to 14 ± 2 m. **Age of feature:** buried twigs in upper part of terrace sequence have calendric ages (based on unpresented ^{14}C ages) within the range 250 AD to 385 BC (2100 ± 250 Cal BP; 99% confidence level)**. Estimated rate(s):** using full calendric age range, dip-slip rate over 2 ka: 2.5 ± 0.5 mm/year, strike slip rate: 6.3 ± 2 mm/year. **Comments:** vertical offset presumably a minimum estimate with unknown but probably small amount of degradation of terrace surface; offset channels post-date by some unknown interval the depositional age of terrace sediments. Although these estimates are therefore minima, it is unlikely that true rates greatly exceed these. **Best estimate:** dip-slip $\geqslant 2.5 \pm$

0.5 mm/year, strike-slip $\geqslant 6.3 \pm 2$ mm/year. **Reference:** Yetton et al. (1998).

Locality 2: Inchbonnie**. Offset feature(s):** between Inchbonnie and Taramakau River, terrace surface is offset vertically by a maximum of 7 m and channels cut on it are dextrally displaced by 11–13 m during two fault displacements. **Age of feature:** weathering rind ages of 1100–1300 years on greywacke clasts within the terrace deposit**. Estimated rate(s):** dextral strike-slip rates 8.5–11.8 mm/year; vertical slip rates 5.4–6.4 mm/year. **Comments:** vertical offset of terrace should be regarded as a minimum estimate with unknown degradation, channel formation would post-date deposition of gravels. **Best estimate:** strike-slip 10 ± 2 mm/year, dip-slip 6 ± 2 mm/year. **Reference:** Berryman et al. (1992).

Locality 3: Toaroha River**. Offset feature(s):** terrace surface offset vertically by 21.75 ± 0.6 m. **Age of feature:** buried fibrous vegetation related to young degradational episode at top surface of terrace gives ^{14}C age of 2730 ± 90 years BP, equivalent to a calendric age of 2382–3102 Cal BP (2σ limits)**. Estimated rate(s):** using full calendric age range, dip-slip rate over 3 ka is 8 ± 1.25 mm/year. **Comments:** Using probability theory, authors provide a refined estimate of 7.8 ± 1 mm/year. **Best estimate:** dip-slip 7.8 ± 1 mm/year. **Reference:** Yetton and Nobes (1998).

Locality 4: Kaka Creek, Mikonui River. **Offset feature(s):** emplacement of crushed mylonite over stream gravels. Overthrusting of 5.0 m perpendicular to strike is bracketed by dated gravel sequences. Amount of movement is minimum due to possibility of erosion during emplacement of younger gravels. **Age of feature:** older (overthrust) gravels: ^{14}C age of 3350 ± 100 years BP; younger unconformable gravels: ^{14}C age of 2600 ± 60 years BP; interval $= 750 \pm 116$ years. **Estimated rate(s):** dip-slip $>6.7 \pm 1$ mm/year. **Comments:** because only a minimum offset can be measured, the rate is a minimum. The dating errors are significant because the difference in dates is only 750 years. **Best estimate:** dip-slip >6.7 mm/year. **Reference:** Rattenbury et al. (1988).

Locality 5: Kakapotahi River. **Offset feature(s):** offset river terraces (post-glacial aggradation surface and younger terrace) and offset risers. **Age of feature:** post-glacial aggradation surface estimated as $13{,}600 \pm 1200$ Cal BP based on ^{14}C ages to north and south of $10{,}800 \pm 150$ and $12{,}290 \pm 90$ years BP (Yetton and Nobes, 1998). Lower surface estimated as 7600 ± 1400 Cal BP by extrapolation. Offset of older and younger risers on east (600 ± 100 m; 250 ± 50 m) and west (375 ± 50 m; 225 ± 25 m) banks give max. and min. estimates of strike-slip, respectively. **Estimated rate(s):** dip-slip 5.9 ± 0.9 mm/year; strike-slip $<44 \pm 8$, $<33 \pm 9$, $>27.5 \pm 5$, $\geqslant 29 \pm 6$ mm/year. **Comments:** error in dip-slip mainly due to uncertainty in age; error in strike-slip due to erosion of terrace risers during displacement plus age uncertainty. Also, calculation ignores any original offset of terrace margin at time of formation. **Best estimate:** dip-slip 6 ± 1 mm/year; strike-slip 29 ± 6 mm/year. **Reference:** Wright et al. (1997); Wright (1998), remeasurement.

Locality 6: Gaunt Creek, Waitangi-taona River. **Offset feature(s):** mylonites thrust over (i) talus fan gravels; (ii) alluvial gravels. **Age of feature:** ^{14}C age of wood in gravel: (i) $12{,}650 \pm 90$ years BP ($14{,}880 \pm 200$ Cal BP); (ii) $10{,}300 \pm 130$ years BP ($12{,}150 \pm 250$ Cal BP). **Estimated rate(s):** dip-slip (i) >12 mm/year; (ii) >9 mm/year; strike-slip (i) $>22 \pm 5$ mm/year; (ii) $>17 \pm 3$ mm/year. **Comments:** measured offsets are dip-slip and are minima due to (i) probable erosion of leading edge of thrust during displacement; (ii) unknown distributed displacement in hanging wall rocks. Strike-slip is calculated from dip-slip using measured striations on fault plane; the mean pitch is $\pm 5°$, which introduces greater uncertainty into the strike-slip estimate. The dates are maximum ages of the overthrust sequences, again providing minimum estimates of rates. The analytical dating error adds little to the uncertainty. The rates have been recalculated using calendric dates. **Best estimate:** dip-slip >12 mm/year; strike-slip >22 mm/year. **Reference:** Cooper and Norris (1994).

Locality 7: Waikukupa River. **Offset feature(s):** emplacement of mylonite over older gravel (1400 m) plus further displacement over younger gravel (150–500 m); calculated internal shortening of thrust sheet (250 m); fault plane striations (trend $070 \pm 5°$); also offset Waikukupa River channel (1500 m since older gravels). **Age of feature:** older fluvio-glacial gravels >40 ka (^{14}C); estimated as 65 ± 5 ka (= Oxygen-isotope stage 4; Suggate, 1990; Martinson et al., 1987); younger gravels correlated with 15 ka Moana Formation. **Estimated rate(s):** net-slip $>24 \pm 2$, $\geqslant 28 \pm 2$, $\geqslant 33 \pm 2$ mm/year; dip-slip $>7 \pm 2.5$, $\geqslant 9.5 \pm 3$ mm/year; strike-slip $>23 \pm 2.5$, $\geqslant 31 \pm 2.5$ mm/year. **Comments:** age uncertainty only gives ± 2 mm/year error, despite lack of direct dating; larger error is in estimating total displacement and is indicated by bracketing estimates. Due to this, error bars in best estimate are not rigorous statistically derived errors, but estimates of uncertainty from range of rates. **Best estimate:** dip-slip 8 ± 3 mm/year; strike-slip 27 ± 5 mm/year. **Reference:** Norris and Cooper (1997).

Locality 8: Paringa River**. Offset feature(s):** uplift of post-glacial marine/terrestrial sedimentary sequence containing lower shell beds and upper peat/forest horizons. **Age of feature:** shells have ^{14}C age of $13{,}400 \pm 150$ years BP (equivalent to a calendric age of 15700 ± 700 Cal BP). Sequence of peat/forest horizons dated between 9630 ± 70 and 3670 ± 40 BP, corresponding to calendric ages of $11{,}000 \pm 500$ and 3870 ± 50 Cal BP, respectively**. Estimated rate(s):** uplift rates, maximum on upthrust ridge (since 16 ka) 13.7 ± 1.0 mm/year; regional uplift rate (since 16 ka) 8.0 ± 1.1 mm/year. On western side of Alpine Fault, two marine terraces 20 km south of Paringa R. (altitude c. 40 m and c. 120 m a.s.l.) have been correlated with the last interglacial (~120 ka) and an earlier interglacial,

respectively (Nathan, 1975), although the only ^{14}C ages are >40 ka. These indicate an uplift rate on the western side of Alpine Fault of < 1 mm/year and probably c. 0.3 mm/year. Dip-slip rate on Alpine Fault at Paringa River is therefore 7–8 mm/year. **Comments:** see detailed discussion of rates in Simpson et al. (1994). **Best estimate:** dip-slip 7.5 ± 1.5 mm/year; uplift rate 8 ± 1 mm/year. **References:** Suggate (1968), Simpson et al. (1994).

Locality 9: North bank, Haast River**. Offset feature(s):** fluvial terrace displaced >9 ± 0.5 m vertically, stream course displaced 94 ± 1 m dextrally. **Age of feature:** youngest wood in terrace sediments has ^{14}C age of 4010 ± 40 years BP (4400 ± 100 Cal BP). **Estimated rate(s):** minimum uplift rate of terrace, relative to downthrown side is >2.0 + 0.2/−0.1 mm/year (assuming terrace formed immediately after deposition of youngest wood). Strike-slip rate >21.3 ± 0.8 mm/year. **Comments:** rates are minima, as the terrace will have formed some time after deposition of youngest wood, and an unknown amount of degradation may have occurred during or prior to uplift. **Best estimate:** dip-slip >2 mm/year; strike slip >21 mm/year. **Reference:** Cooper and Norris (1995).

Locality 10: South bank, Haast River**. Offset feature(s):** river terrace surface offset vertically by c. 2 m, buried channel edge displaced dextrally by 25 ± 1 m. **Age of feature:** terrace offsets are inferred from trench stratigraphy to result from three earthquake events, the oldest occurring immediately prior to sediments containing seeds that have a ^{14}C age of 850 ± 50 years BP (equivalent to calendric age of 740 ± 50 Cal BP)**. Estimated rate(s):** dip-slip 2–2.5 mm/year; strike-slip 28 ± 4 mm/year. **Comments:** uncertainties arise from time between first event and dated sediments (probably <50 years) and timing of the next event (this becomes important due to relatively short time interval)—the longer it is, the lower the calculated rate. In calculating uncertainty, we assume the next event occurs by 2050 ± 50 AD (see Yetton et al., 1998). These considerations result in an estimated time period of 890 ± 120 years. **Best estimate:** dip-slip 2.25 ± 0.5 mm/year; strike slip 28 ± 4 mm/year. **Reference:** Berryman et al. (1998).

Locality 11: Okuru River**. Offset feature(s):** uplift of fossiliferous sediments. **Age of feature:** shells have ^{14}C age of 9740 ± 200 years BP (10,960 + 113/−411 Cal BP)**. Estimated rate(s):** original uplift rate relative to sea level calculated at 4.9 mm/year, but more recent estimates of sea level rise since deposition result in revised rate of 4.0 ± 0.2 mm/year**. Comments:** shells deposited close to sea level, now at 13 ± 1 m a.s.l. Sea level rise since 9740 ± 200 years BP originally estimated at 35 m; more recent determinations suggest rise of 28 m since 9940 years BP or 24 m since 9540 years BP (Gibb, 1986). **Best estimate:** uplift rate relative to sea level 4.0 ± 0.2 mm/year; assuming a maximum rate of uplift of the western side of <1 mm/year (see locality 8), dip-slip = 3 ± 0.5 mm/year. **Reference:** Cooper and Bishop (1979).

Locality 12: Hokuri Creek. **Offset feature(s):** offset moraine, uplifted shells, horizontal fault plane striations. **Age of feature:** moraine of last advance of last glaciation estimated as 17 ± 2 ka; shells have ^{14}C age of 6490 ± 90 years BP. **Estimated rate(s):** strike-slip 26 ± 6 mm/year; uplift (west of fault) 1.4 ± 0.5 mm/year; dip-slip 0–1 mm/year up to west. **Comments:** striations and offset small channels clearly show near zero dip-slip; uplift may be local value only. **Best estimate:** dip-slip 0 mm/year; strike-slip 26 ± 6 mm/year; uplift to west 1.4 ± 0.5 mm/year**. Reference:** Sutherland and Norris (1995).

Locality 13: Lake McKerrow. **Offset feature(s):** offset walls of glacially excavated lake-filled valley. Intertidal shell beds 5–8 m above MSL northwest and 4.3–6.4 m above MSL southeast of Alpine Fault. **Age of feature:** glacial lake silts have ^{14}C age of 13,120 ± 110 years BP (15,600 ± 110 Cal BP). Shell beds northwest of fault have ^{14}C ages of 3500–8000 years BP; those southeast of fault have ages 7800–8100 years BP. **Estimated rate(s):** strike-slip 26 ± 7 mm/year; uplift 2.2 ± 0.2 mm/year northwest of fault, 1.6 ± 0.3 mm/year southeast of fault. **Best estimate:** strike-slip 26 ± 7 mm/year; dip-slip <1 mm/year; uplift 2.2 ± 0.2 mm/year to northwest, 1.6 ± 0.3 mm/year to southeast. **References:** Hull and Berryman (1986), Sutherland and Norris (1995).

References

Adams, J., 1980. Contemporary uplift and erosion of the Southern Alps, New Zealand. Geological Society of America Bulletin 91, 1–114.

Anderson, H.J., Webb, T., 1994. New Zealand seismicity: patterns revealed by the upgraded National Seismograph Network. New Zealand Journal of Geology and Geophysics 37, 477–493.

Anderson, H.J., Webb, T., Jackson, J., 1993. Focal mechanisms of large earthquakes in the South Island of New Zealand: implications for the accommodation of Pacific–Australia plate motion. Geophysical Journal International 115, 1032–1054.

Bard, E., Hamelin, B., Fairbanks, R.G., Zindler, A., 1990. Calibration of the C^{14} timescale over the past 30,000 yrs using mass spectrometric U–Th ages on Barbados corals. Nature 345, 405–409.

Bard, E., Arnold, M., Fairbanks, R.G., Hamelin, B., 1993. Th^{230}–U^{234} and C^{14} ages obtained by mass spectrometry on corals. Radiocarbon 35, 191–199.

Barnes, P., Davy, B., Sutherland, R., Delteil, J., 1999. Structures and sedimentation of the very obliquely convergent lower Fiordland margin. New Zealand Geophysical Society Annual Conference, Wellington, Abstract Volume, Tec 10.

Beavan, J., Moore, M., Pearson, C., Henderson, M., Parsons, B., Bourne, S., England, P., Walcott, D., Blick, G., Darby, D., Hodgkinson, K., 1999. Crustal deformation during 1994–1998 due to oblique continental collision in the central Southern Alps, New Zealand, and implications for seismic potential of the Alpine fault. Journal of Geophysical Research 104, 25232–25255.

Benson, W.N., 1952. Meeting of the Geological Division of the Pacific Science Congress in New Zealand, February, 1949. International Proceedings of the Geological Society of America 11, 11–13.

Berryman, K.R., Beanland, S., Cooper, A.F., Cutten, H.N., Norris, R.J., Wood, P.R., 1992. The Alpine Fault, New Zealand: variation in Quaternary tectonic style and geomorphic expression. Annales Tectonicae VI, 126–163.

Berryman, K., Cooper, A.F., Norris, R.J., Sutherland, R., Villamor, P., 1998. Paleoseismic investigation of the Alpine Fault at Haast and

Okuru. Geological Society of New Zealand Miscellaneous Publication 101A, 44.

Bibby, H.M., Haines, A.J., Walcott, R.I., 1986. Geodetic strain and the present day plate boundary zone through New Zealand. In: Reilly, W.I., Harford, B.E. (Eds.), Recent Crustal Movements of the Pacific Region. Royal Society of New Zealand Bulletin 24, pp. 427–438.

Bishop, D.G., 1991. High-level marine terraces in western and southern New Zealand: indicators of the tectonic tempo of an active continental margin. Society of Economic Paleontologists and Mineralogists Special Publication 12, 69–78.

Bishop, D.G., 1994. Extent and regional deformation of the Otago peneplain. Institute of Geological and Nuclear Sciences Science Report 94/1.

Braun, J., Beaumont, C., 1995. Three-dimensional numerical experiments of strain partitioning at oblique plate boundaries: implications for contrasting tectonic styles in the southern Coast Ranges, California, and central South Island, New Zealand. Journal of Geophysical Research 100, 18059–18074.

Bull, W.B., Cooper, A.F., 1986. Uplifted marine terraces along the Alpine fault, New Zealand. Science 234, 1225–1228.

Cobbold, P.R., Gapais, D., Rosello, E.A., 1991. Partitioning of transpressive motions within a sigmoidal foldbelt: the Variscan Sierras Australes, Argentina. Journal of Structural Geology 13, 777–786.

Cooper, A.F., 1980. Retrograde alteration of chromium kyanite in metachert and amphibolite whiteschist from the Southern Alps, New Zealand, with implications for uplift on the Alpine Fault. Contributions to Mineralogy and Petrology 75, 153–164.

Cooper, A.F., Bishop, D.G., 1979. Uplift rates and high level marine platforms associated with the Alpine fault at Okuru River, south Westland. In: Walcott, R.I., Cresswell, M.M. (Eds.), The Origin of the Southern Alps. Royal Society of New Zealand Bulletin 18, pp. 35–43.

Cooper, A.F., Norris, R.J., 1994. Anatomy, structural evolution and slip rate of a plate-boundary thrust: the Alpine fault at Gaunt Creek, Westland, New Zealand. Geological Society of America Bulletin 106, 627–633.

Cooper, A.F., Norris, R.J., 1995. Displacement on the Alpine Fault at Haast River, South Westland, New Zealand. New Zealand Journal of Geology and Geophysics 38, 509–514.

Cowan, H.A., McGlone, M.S., 1991. Late Holocene displacements and characteristic earthquakes on the Hope River segment of the Hope Fault, New Zealand. Journal of the Royal Society of New Zealand 21, 373–384.

Cox, S.C., Findlay, R.H., 1995. The Main Divide Fault Zone and its role in formation of the Southern Alps. New Zealand Journal of Geology and Geophysics 38, 489–499.

Cutress, G., Herzer, R.H., Wood, R., Detteil, J., Lebrun, J.-F. and GEODYNZ team, 1998. Fiordland offshore geology: integrated swath mapping and geophysics. Folio Series 3, Institute of Geological and Nuclear Sciences, Wellington.

Davey, F.J., Smith, E.G.C., 1983. The tectonic setting of the Fiordland region, south-west New Zealand. Geophysical Journal of the Royal Astronomical Society 72, 23–38.

Davey, F.J., Henyey, T., Kleffmann, S., Melhuish, A., Okaya, D., Stern, T.A., Woodward, D.J., 1995. Crustal reflections from the Alpine Fault zone, South Island, New Zealand. New Zealand Journal of Geology and Geophysics 38, 601–604.

Davey, F.J., Henyey, T., Holbrook, W.S., Okaya, D., Stern, T.A., Melhuish, A., Henrys, S., Anderson, H., Eberhart-Phillips, D., McEvilly, T., Uhrhammer, R., Wu, F., Jiracek, G.R., Wannamaker, P.E., Caldwell, G., Christensen, N., 1998. Preliminary results from a geophysical study across a modern continent–continent collisional plate boundary—the Southern Alps, New Zealand. Tectonophysics 288, 221–235.

Delteil, J., Collot, J.-Y., Wood, R., Herzer, R., Calmant, S., Christoffel, D., Coffin, M., Ferriere, J., Lamarche, G., Lebrun, J.-F., Mauffret, A., Pontoise, B., Popoff, M., Ruellan, E., Sosson, M., Sutherland, R., 1996. From strike-slip faulting to oblique subduction: a survey of the Alpine Fault–Puysegur Trench transition, New Zealand, results of Cruise Geodynz-sud Leg 2. Marine Geophysical Researches 18, 383–399.

DeMets, C., Gordon, R.G., Argus, D.F., Stein, S., 1994. Effect of recent revisions to the geomagnetic reversal time scale on estimates of current plate motions. Geophysical Research Letters 21, 2191–2194.

Eberhart-Phillips, D., 1995. Examination of seismicity in the central Alpine Fault region, South Island, New Zealand. New Zealand Journal of Geology and Geophysics 38, 571–578.

Fitch, T.J., 1972. Plate convergence, transcurrent faults, and internal deformation adjacent to southeast Asia and the western Pacific. Journal of Geophysical Research 77, 4432–4460.

Gibb, J.G., 1986. A New Zealand regional Holocene eustatic sea-level curve and its application to determination of vertical tectonic movements. Royal Society of New Zealand Bulletin 24, 377–395.

Grapes, R.H., Watanabe, T., 1992. Metamorphism and uplift of Alpine Schist in the Franz Josef–Fox Glacier area of the Southern Alps, New Zealand. Journal of Metamorphic Geology 10, 171–180.

Grapes, R.H., Watanabe, T., 1994. Mineral composition variation in Alpine Schist, Southern Alps, New Zealand: implications for recrystallization and exhumation. The Island Arc 3, 163–181.

Henderson, M., Pearson, C., Koons, P.O., 1999. Horizontal velocities in the South Island, New Zealand, from analysis of GPS and terrestrial survey measurements. New Zealand Geophysical Society Annual Conference Proceedings, Abstract volume, Tec 9.

Holdsworth, R.E., Strachan, R.A., 1991. Interlinked system of ductile strike-slip and thrusting formed by Caledonian sinistral transpression in northeastern Greenland. Geology 19, 510–513.

Hull, A.G., Berryman, K.R., 1986. Holocene tectonism in the region of the Alpine fault at Lake McKerrow, Fiordland, New Zealand. In: Reilly, W.I., Harford, B.E. (Eds.), Recent Crustal Movements of the Pacific Region. Royal Society of New Zealand Bulletin 24, pp. 317–331.

Jackson, J.A., Norris, R.J., Youngson, J.H., 1996. The structural evolution of active fault and fold systems in central Otago, New Zealand: evidence revealed by drainage patterns. Journal of Structural Geology 18, 217–235.

Jones, C.H., Wesnousky, S.G., 1992. Variations in strength and slip rate along the San Andreas Fault System. Science 256, 83–86.

Koons, P.O., 1987. Some thermal and mechanical consequences of rapid uplift: an example from the Southern Alps, New Zealand. Earth and Planetary Science Letters 86, 307–319.

Koons, P.O., 1990. Two-sided orogen: collision and erosion from the sandbox to the Southern Alps, New Zealand. Geology 18, 679–683.

Koons, P.O., 1994. Three-dimensional critical wedges: tectonics and topography in oblique collisional orogens. Journal of Geophysical Research 99, 12301–12315.

Koons, P.O., 1995. Modeling the topographic evolution of collisional belts. Annual Reviews of Earth and Planetary Science 23, 375–408.

Koons, P.O., Norris, R.J., Cooper, A.F., Craw, D., 1998. Mechanics of a single structure accommodating oblique convergence: the development of the Alpine Fault. Geological Society of New Zealand Miscellaneous Publication 101A, 138.

Larson, K.M., Fraymuller, J., 1995. Relative motions of the Australian, Pacific and Antarctic plates estimated by the Global Positioning System. Geophysical Research Letters 22, 37–40.

Lensen, G.J., 1964. The general case of progressive fault displacement of flights of degradational terraces. New Zealand Journal of Geology and Geophysics 7, 864–870.

Lensen, G.J., 1968. Analysis of progressive fault displacement during downcutting at Branch River terraces, South Island, New Zealand. Geological Society of America Bulletin 79, 545–556.

Markley, M., Norris, R.J., 1999. Structure and neotectonics of the Blackstone Hill Antiform, central Otago, New Zealand. New Zealand Journal of Geology and Geophysics 42, 205–218.

Martinson, D.G., Pisias, N.G., Hays, J.D., Imbrie, J., Moore Jr., T.C., Shackleton, N.J., 1987. Age dating and orbital theory of ice ages: development of a high-resolution 0–300,000 year chronology. Quaternary Research 27, 1–29.

McCaffrey, R., 1991. Slip vectors and stretching of the Sumatran forearc. Geology 19, 881–884.

McCaffrey, R., 1992. Oblique plate convergence, slip vectors, and forearc deformation. Journal of Geophysical Research 97, 8905–8915.

Molnar, P., 1992. Brace–Goetze strength profiles, the partitioning of strike-slip and thrust faulting at zones of oblique convergence, and the stress–heat flow paradox of the San Andreas Fault. In: Evans, B., Wong, T.-F. (Eds.), Fault Mechanics and Transport Properties of Rocks. Academic Press, London, pp. 435–460.

Nathan, S., 1975. Late Quaternary terraces between Ship Creek and the Whakapohai River, South Westland, New Zealand. Journal of the Royal Society of New Zealand 5, 313–327.

Nathan, S., Anderson, H.J., Cook, R.A., Herzer, R.H., Hoskins, R.H., Raine, J.I., Smale, D., 1986. Cretaceous and Cenozoic sedimentary basins of the West Coast Region, South Island, New Zealand. New Zealand Geological Survey Basin Studies 1, Department of Scientific and Industrial Research, Wellington.

Norris, R.J., Cooper, A.F., 1986. Small-scale fractures, glaciated surfaces, and recent strain adjacent to the Alpine fault, New Zealand. Geology 14, 687–690.

Norris, R.J., Cooper, A.F., 1995. Origin of small-scale segmentation and transpressional thrusting along the Alpine fault, New Zealand. Geological Society of America Bulletin 107, 231–240.

Norris, R.J., Cooper, A.F., 1997. Erosional control on the structural evolution of a transpressional thrust complex on the Alpine Fault, New Zealand. Journal of Structural Geology 19, 1323–1342.

Norris, R.J., Koons, P.O., Cooper, A.F., 1990. The obliquely-convergent plate boundary in the South Island of New Zealand: implications for ancient collision zones. Journal of Structural Geology 12, 715–725.

Pearson, C., 1994. Geodetic strain determinations from the Okarito and Godley–Tekapo regions, central South Island, New Zealand. New Zealand Journal of Geology and Geophysics 37, 309–318.

Pillans, B., 1990. Pleistocene marine terraces in New Zealand: a review. New Zealand Journal of Geology and Geophysics 33, 219–232.

Platt, J.P., 1993. Mechanics of oblique convergence. Journal of Geophysical Research 98, 16239–16256.

Rattenbury, M.S., Cooper, A.F., Norris, R.J., 1988. Recent Alpine Fault thrusting at Kaka Creek, central Westland, New Zealand. New Zealand Journal of Geology and Geophysics 31, 117–120.

Sibson, R.H., White, S.H., Atkinson, B.K., 1979. Fault rock distribution and structure within the Alpine Fault Zone: a preliminary account. In: Walcott, R.I., Cresswell, M.M. (Eds.), The Origin of the Southern Alps. Bulletin of the Royal Society of New Zealand 18, pp. 55–65.

Simpson, G.D.H., Cooper, A.F., Norris, R.J., 1994. Late Quaternary evolution of the Alpine fault zone at Paringa, South Westland. New Zealand Journal of Geology and Geophysics 37, 49–58.

Stuiver, M., Becker, B., 1993. High precision decadal calibration of the radiocarbon timescale, AD 1950–6000 BC. Radiocarbon 35, 35–65.

Stuiver, M., Reimer, P.J., 1993. Extended ^{14}C database and revised CALIB 3.0 C age calibration programme. Radiocarbon 35, 215–230.

Suggate, R.P., 1963. The Alpine fault. Transactions of the Royal Society of New Zealand 2, 105–129.

Suggate, R.P., 1968. The Paringa Formation, Westland, New Zealand. New Zealand Journal of Geology and Geophysics 11, 345–355.

Suggate, R.P., 1990. Late Pliocene and Quaternary glaciations of New Zealand. Quaternary Science Reviews 9, 175–197.

Sutherland, R., 1994. Displacement since the Pliocene along the southern section of the Alpine fault, New Zealand. Geology 22, 327–331.

Sutherland, R., 1995. Late Cenozoic tectonics in the SW Pacific, and development of the Alpine Fault through southern South Island, New Zealand. Ph.D. thesis, University of Otago, Dunedin, New Zealand.

Sutherland, R., Norris, R.J., 1995. Late Quaternary displacement rate, paleoseismicity, and geomorphic evolution of the Alpine Fault: evidence from Hokuri Creek, South Westland, New Zealand. New Zealand Journal of Geology and Geophysics 38, 419–430.

Teyssier, C., Tikoff, B., Markely, M., 1995. Oblique plate motion and continental tectonics. Geology 23, 447–450.

Tikoff, B., Teyssier, C., 1994. Strain modeling of displacement–field partitioning in transpressional orogens. Journal of Structural Geology 16, 1575–1588.

Tippett, J.M., Kamp, P.J.J., 1993. Fission track analysis of the late Cenozoic vertical kinematics of continental Pacific crust, South Island, New Zealand. Journal of Geophysical Research 98, 16119–16148.

Tregoning, P., Lambeck, K., Stolz, A., Morgan, P., McClusky, S.C., van der Beek, P., McQueen, H., Jackson, R.J., Little, R.P., Laing, A., Murphy, B., 1998. Estimation of current plate motions in Papua New Guinea from Global Positioning System observations. Journal of Geophysical Research 103, 12181–12203.

Van Dissen, R.J., Hull, A.G., Read, S.A.L., 1993. Timing of some large Holocene earthquakes on the Ostler Fault, New Zealand. Proceedings of the CRCM '93, Kobe, Japan, pp. 381–386.

Walcott, R.I., 1978a. Present tectonics and late Cenozoic evolution of New Zealand. Geophysical Journal of the Royal Astronomical Society 52, 137–164.

Walcott, R.I., 1978b. Geodetic strains and large earthquakes in the axial tectonic belt of North Island, New Zealand. Journal of Geophysical Research 83, 19–29.

Walcott, R.I., 1998. Modes of oblique compression: late Cenozoic tectonics of the South Island, New Zealand. Reviews of Geophysics 36, 1–26.

Ward, C.M., 1988. New Zealand marine terraces: uplift rates. Science 240, 803.

Warren, G., 1967. Sheet 17 Hokitika (1st ed.). Geological Map of New Zealand 1:250,000, Department of Scientific and Industrial Research, Wellington.

Wellman, H.W., 1953. Data for the study of Recent and late Pleistocene faulting in the South Island of New Zealand. New Zealand Journal of Science and Technology 34B, 270–288.

Wellman, H.W., 1955. New Zealand Quaternary tectonics. Geologische Rundschau 43, 248–257.

Wellman, H.W., 1979. An uplift map for the South Island of New Zealand, and a model for uplift of the Southern Alps. In: Walcott, R.I., Cresswell, M.M. (Eds.), The Origin of the Southern Alps. Bulletin of the Royal Society of New Zealand 18, pp. 13–20.

Wellman, H.W., Willett, R.W., 1942. The geology of the West Coast from Abut Head to Milford Sound—Part 1. Transactions of the Royal Society of New Zealand 71, 282–306.

Wells, A., Yetton, M.D., Duncan, R.P., Stewart, G.H., 1999. Prehistoric dates of the most recent Alpine fault earthquakes, New Zealand. Geology 27, 995–998.

Wright, C.A., 1998. Geology and paleoseismicity of the central Alpine Fault, New Zealand. MSc thesis, University of Otago, Dunedin, New Zealand.

Wright, C.A., Norris, R.J., Cooper, A.F., 1997. Mapping of the Central Alpine Fault, Stage 1: Mikonui to Waitaha Rivers, Westland. Geological Society of New Zealand Miscellaneous Publication 95A, 172.

Yeats, R.S., 1987. Tectonic map of central Otago based on Landsat imagery. New Zealand Journal of Geology and Geophysics 30, 261–271.

Yeats, R.S., Berryman, K.R., 1987. South Island, New Zealand and Transverse Ranges, California: a seismotectonic comparison. Tectonics 6, 363–376.

Yetton, M.D., Nobes, D.C., 1998. Recent vertical offset and near-surface structure of the Alpine Fault in Westland, New Zealand, from ground penetrating radar profiling. New Zealand Journal of Geology and Geophysics 41, 485–492.

Yetton, M.D., Wells, A., Traylen, N.J., 1998. The probabilities and consequences of the next Alpine Fault earthquake. EQC, Research Report 95/193.

Youngson, J.H., Craw, D., Landis, C.A., Schmitt, K.R., 1998. Redefinition and interpretation of late Miocene–Pleistocene terrestrial stratigraphy, Central Otago, New Zealand. New Zealand Journal of Geology and Geophysics 41, 51–68.